Electronic Supplementary Material (ESI) for Dalton Transactions.

Supporting information

Visible detection of copper ions via fluorescent probe based on red carbon dots and zirconium metal-organic frameworks

Jing-Xing Wu and Bing Yan*

School of Chemical Science and Engineering, Tongji University, Siping Road 1239, Shanghai 200092, China.

E-mail: byan@tongji.edu.cn.

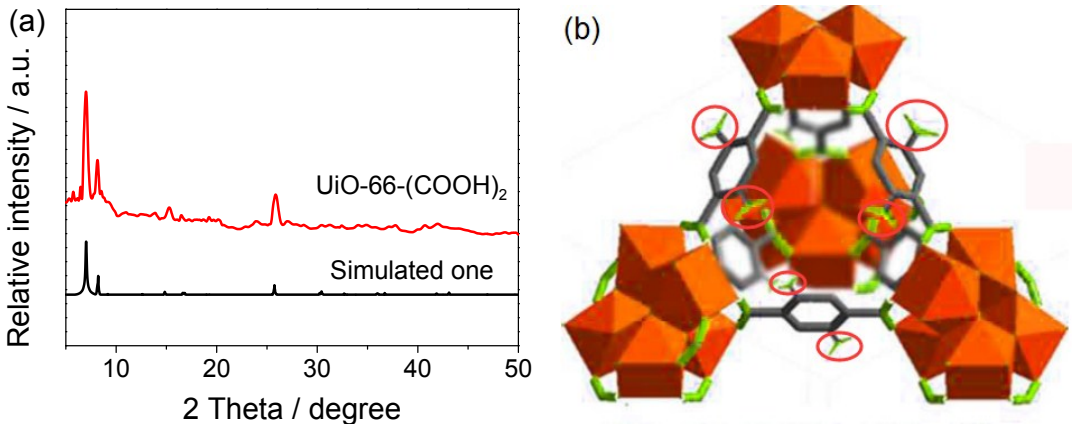

Fig. S1 (a) PXRD patterns of the UiO-66-$(COOH)_2$ (red) and simulated one (black); (b) representative structure of UiO-66-$(COOH)_2$. Dark gray, green represent C and O atoms, respectively.

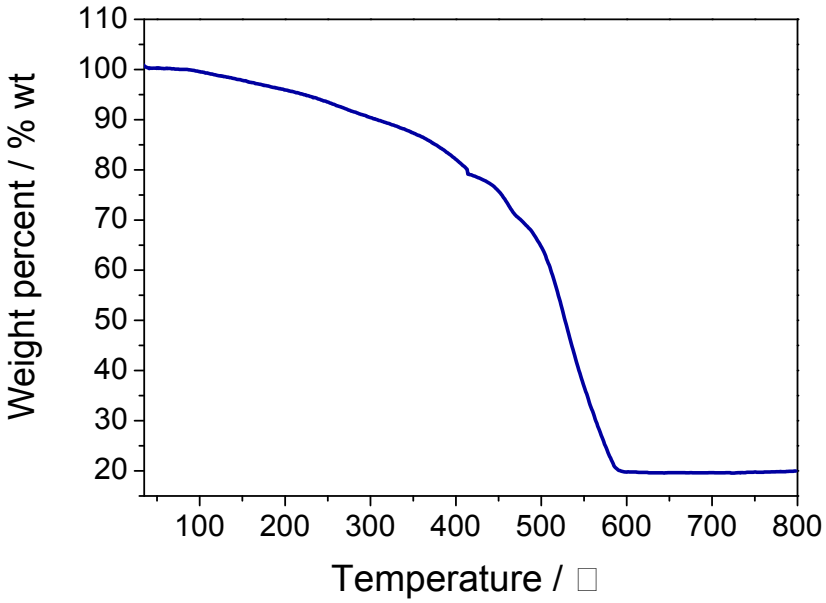

Fig. S2 Thermogravimetric analysis of UiO-66-$(COOH)_2$.

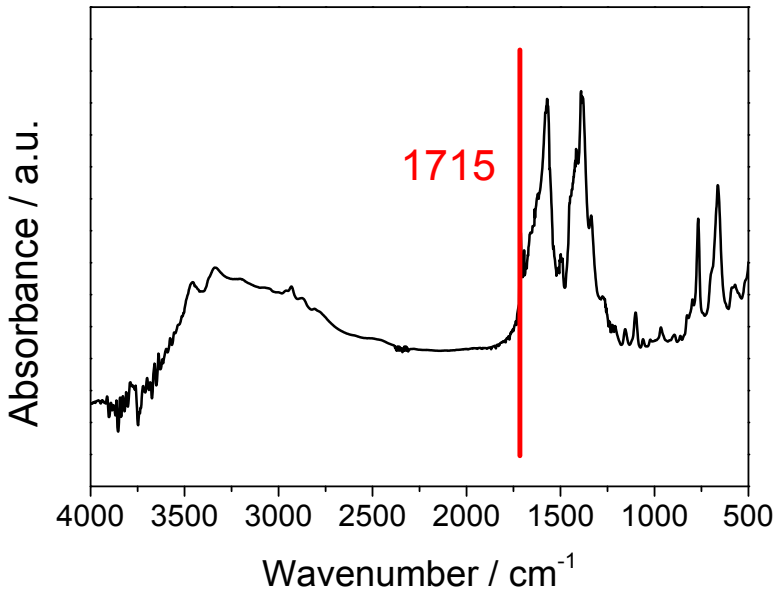

Fig. S3 FTIR spectra of UiO-66-$(COOH)_2$.

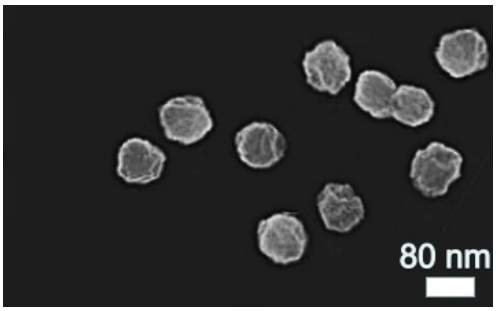

Fig. S4 SEM image of UiO-66-$(COOH)_2$

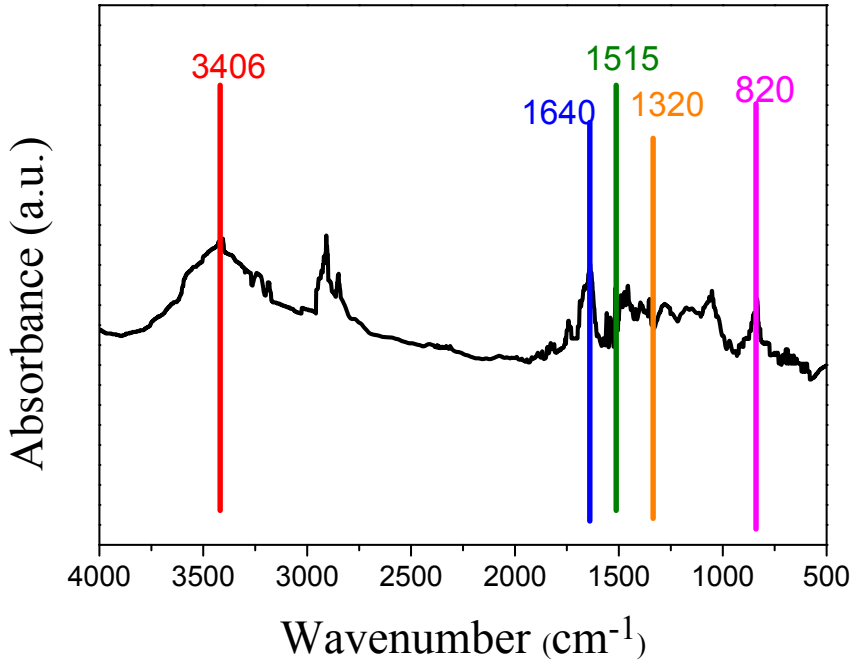

Fig. S5 FTIR spectra of R-BF-CQDs.

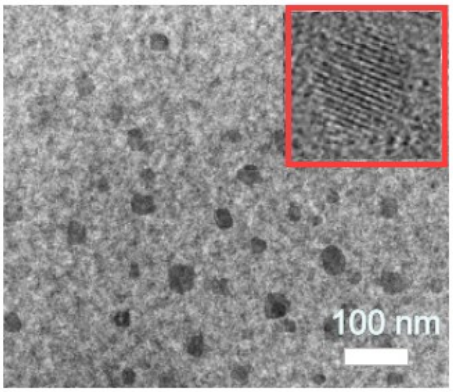

Fig. S6 TEM and HRTEM (inset) images of R-BF-CQDs.

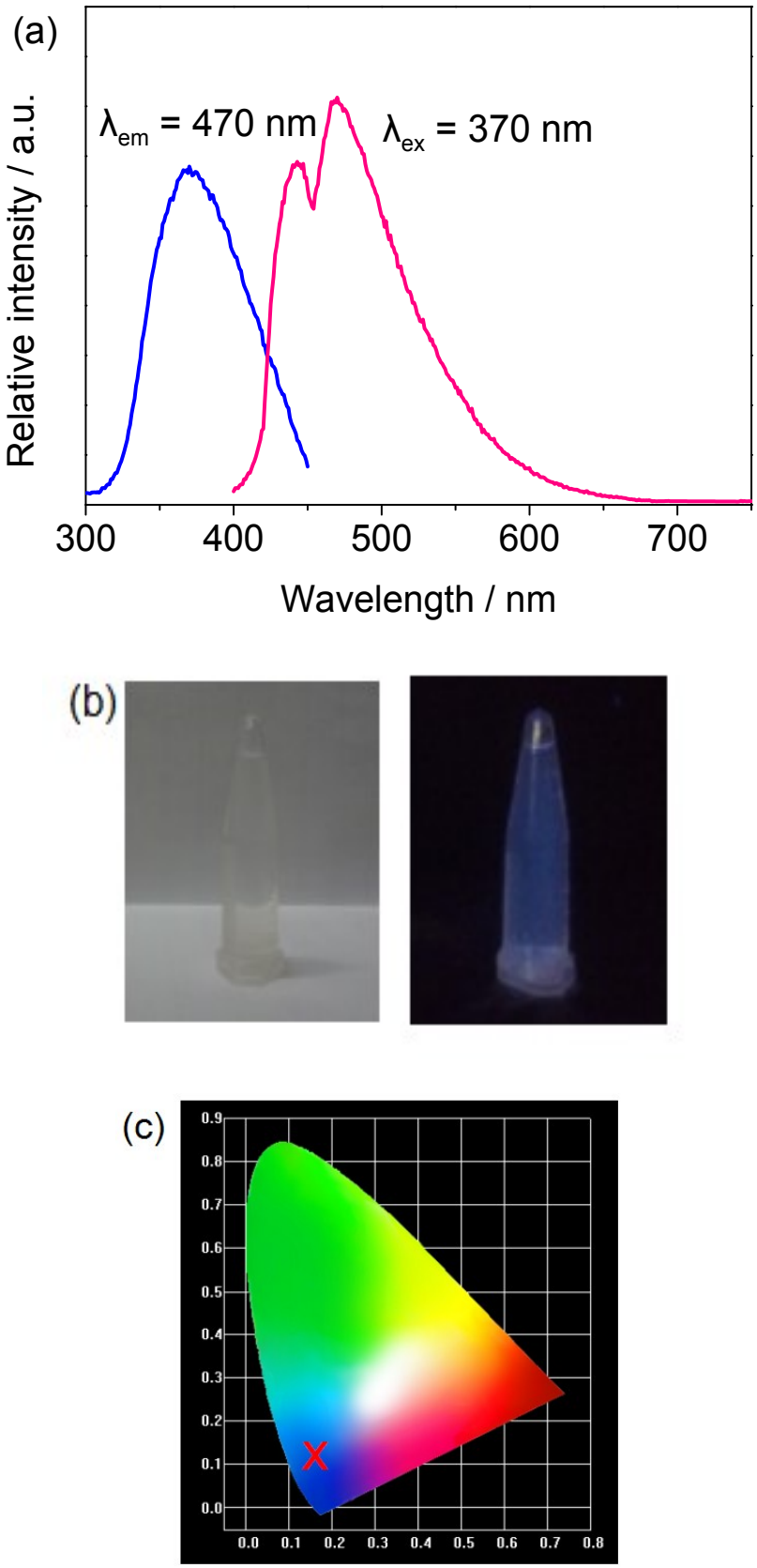

Fig. S7 (a) The excitation (blue) and emission spectra (pink) of UiO-66-$(COOH)_2$ samples dispersed in aqueous solution; (b) Corresponding photographs of UiO-66-$(COOH)_2$ in aqueous solution under daylight and UV light at 365 nm; (c) the CIE chromaticity diagram of UiO-66-$(COOH)_2$ excited at 370 nm (X = 0.16, Y = 0.13).

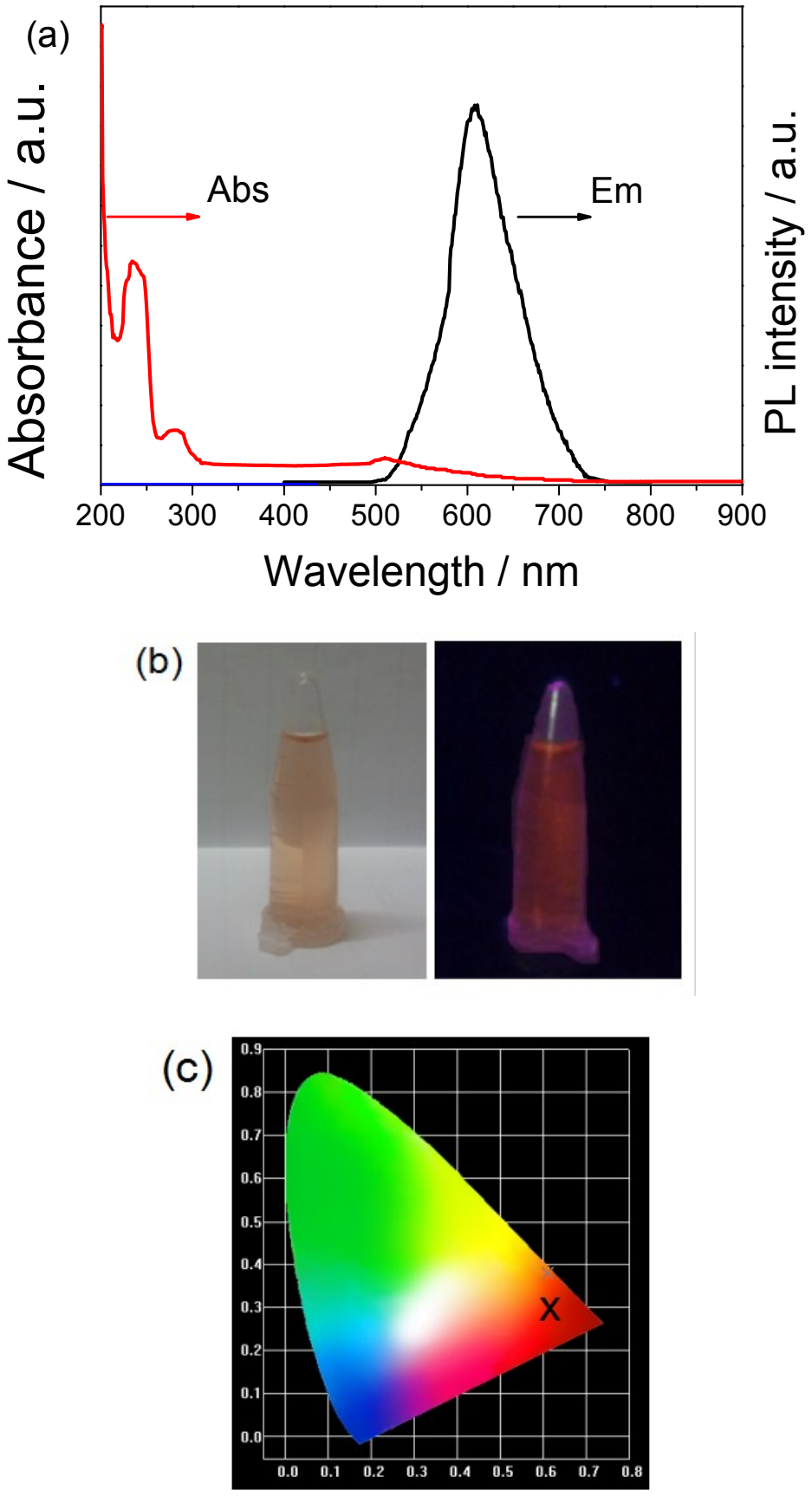

Fig. S8 (a) UV−vis absorbance (red) and emission spectra (black) of R-BF-CQDs samples dispersed in aqueous solution; (b) Corresponding photographs of R-BF-CQDs in aqueous solution under daylight and UV light at 365 nm; (c) the CIE chromaticity diagram of R-BF-CQDs excited at 370 nm (X = 0.61, 0.31).

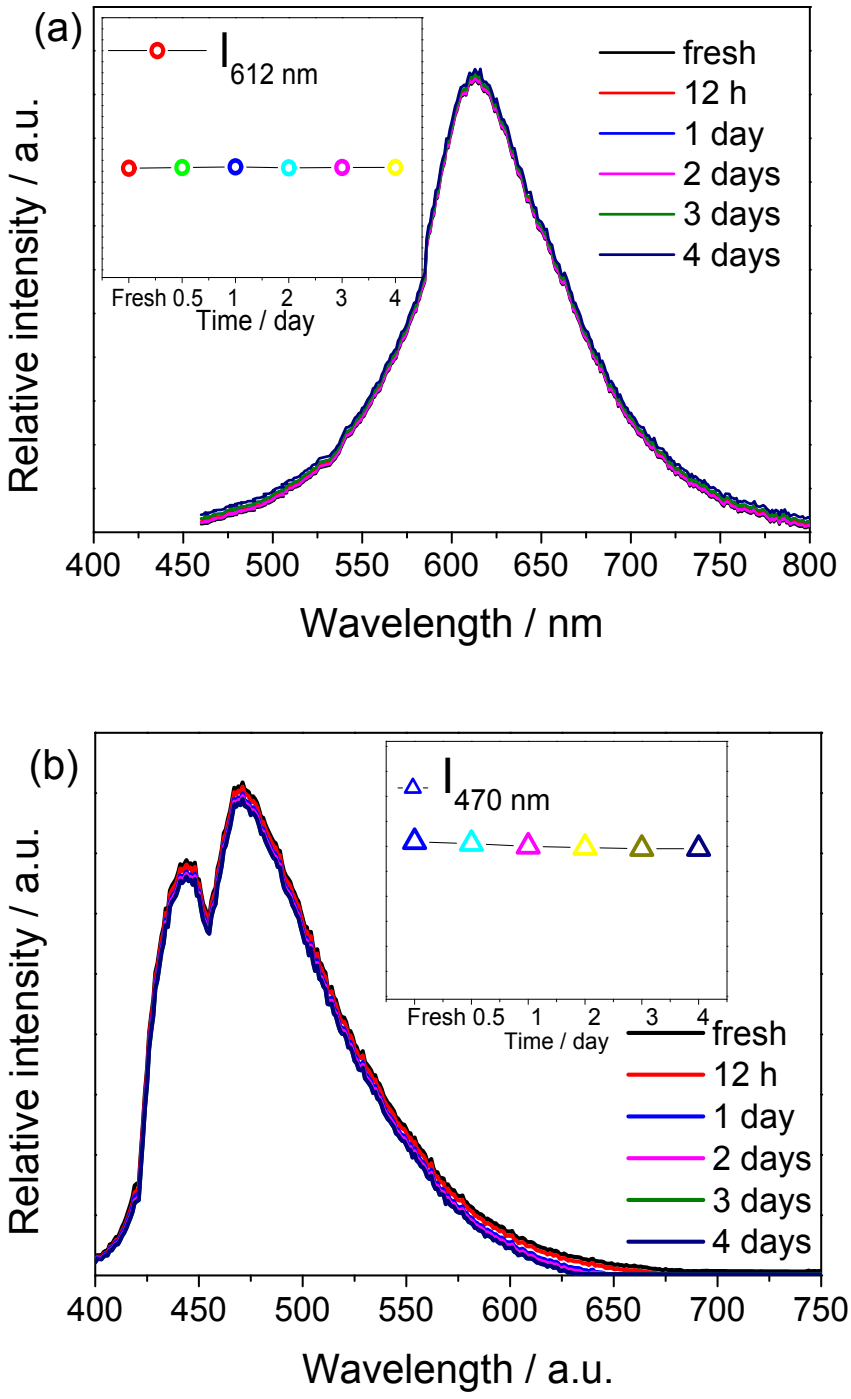

Fig. S9 Day-to-day fluorescence stability of (a) UiO-66-$(COOH)_2$ and (b) R-BF-CQDs after immersing in aqueous solution for several days and the inset of a is the corresponding relative intensity at λ_{em} = 612 nm while the inset of b is at λ_{em} = 470 nm.

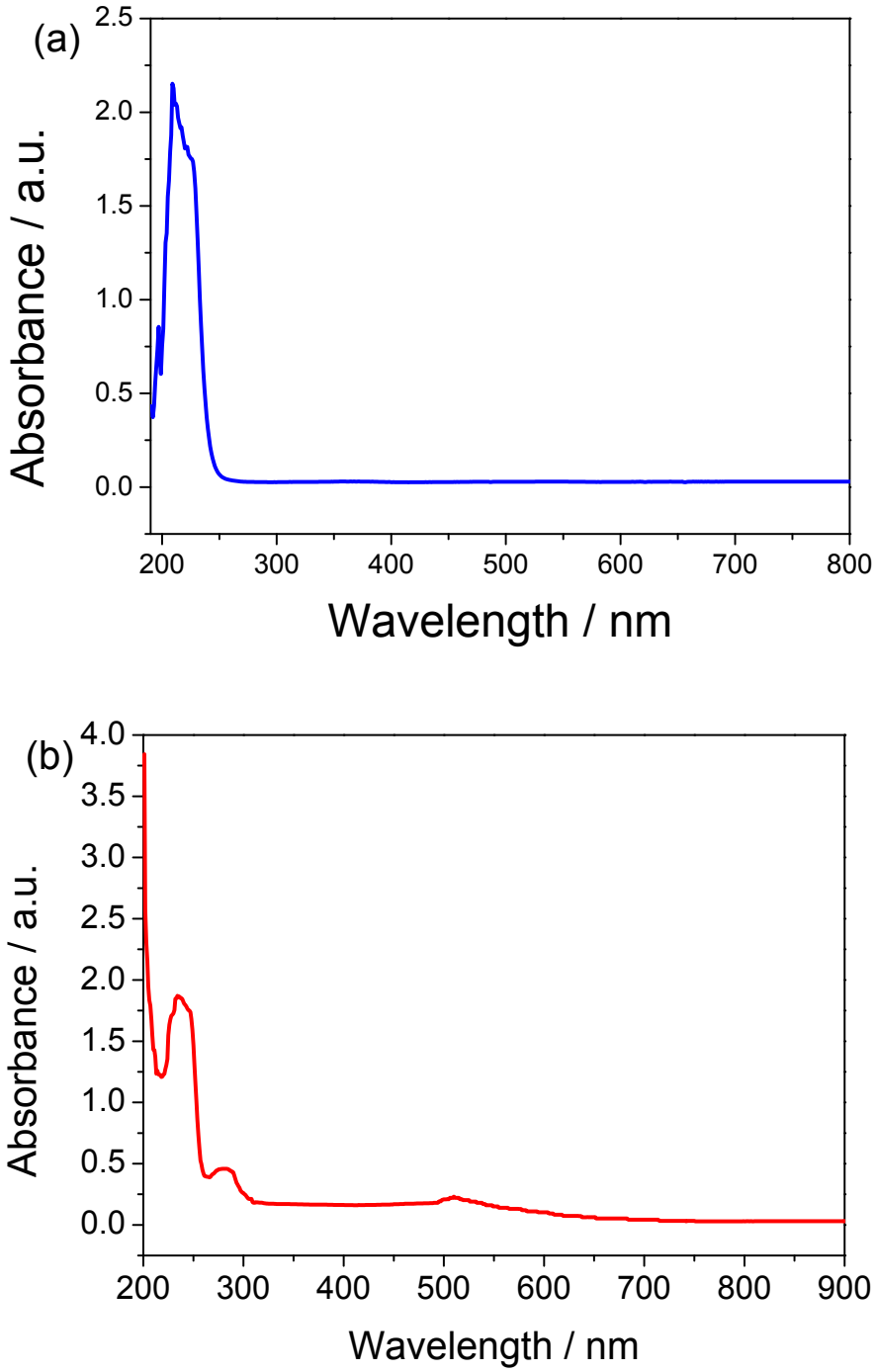

Fig. S10 UV−vis absorption spectra of suspended UiO-66-$(COOH)^2$ (a) and R-BF-CQDs in H_2O solution.

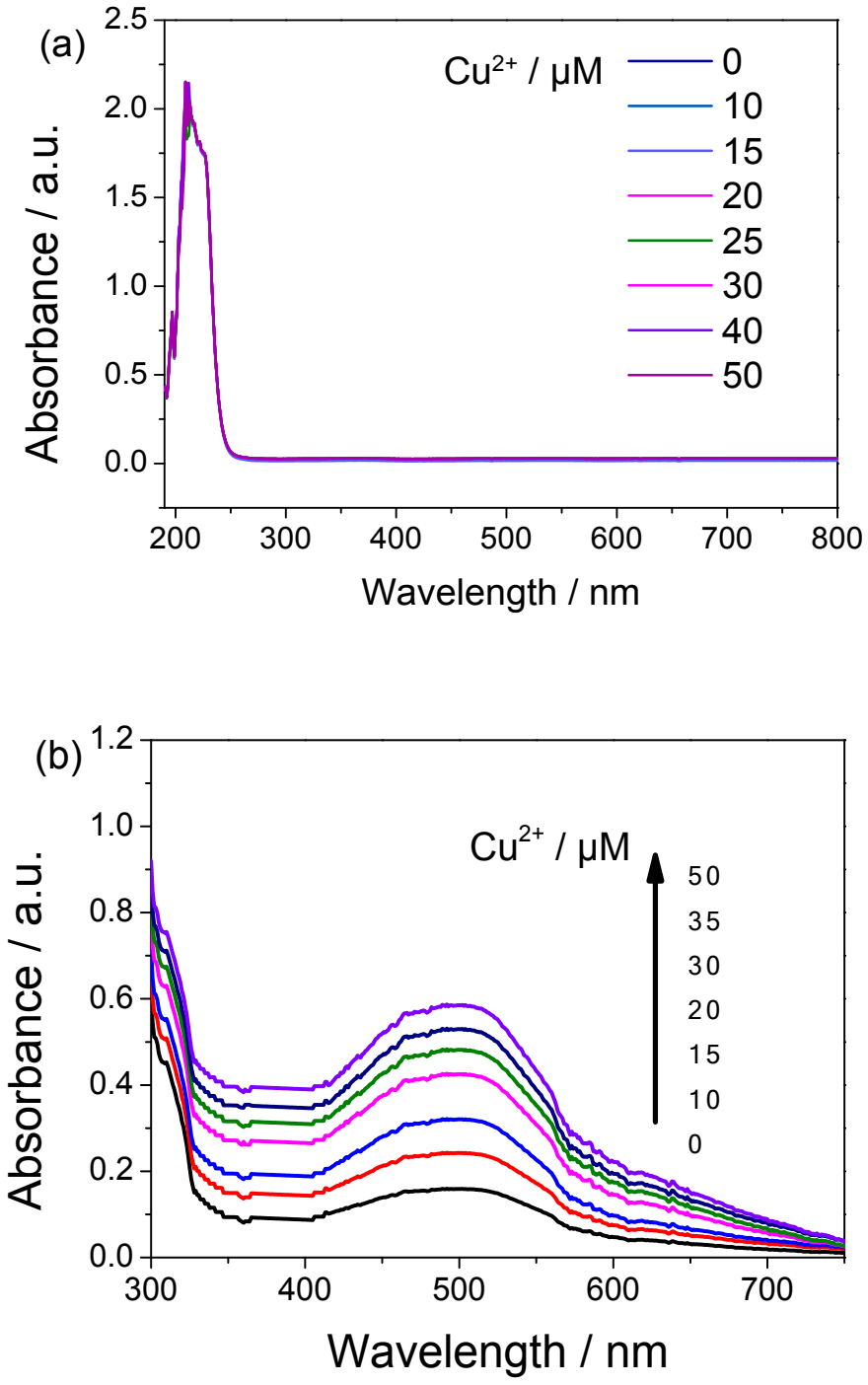

Fig. S11 Evolutions of UV–vis spectra of UiO-66-$(COOH)_2$ (a) and R-BF-CQDs (b) after the addition of Cu^{2+}

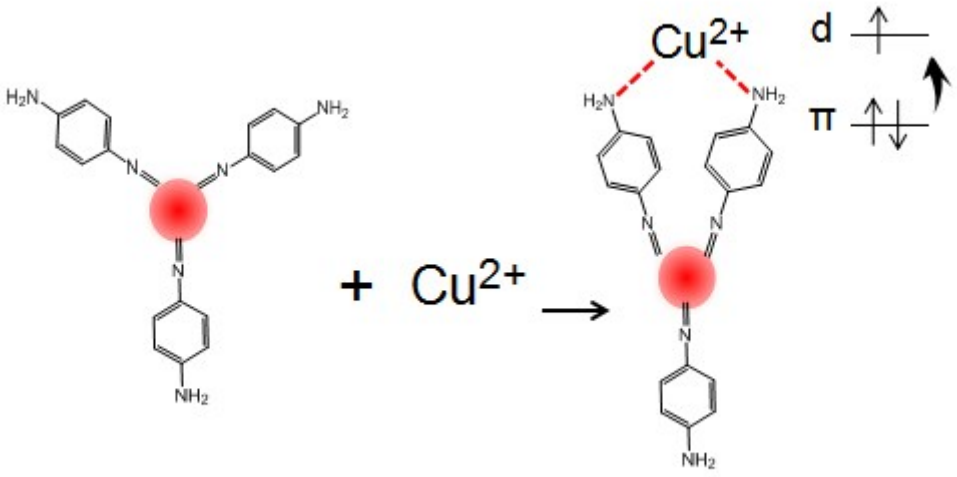

Fig. S12 Scheme of ligand-to-metal charge transfer between R-BF-CQDs and Cu^{2+} ions.

Table S1 The ICP-MS results of **a** Cu^{2+}+UiO-66-$(COOH)_2$, **b** Cu^{2+}+R-BF-CQDs and **c** Cu^{2+}+UiO-66-$(COOH)_2$+R-BF-CQDs

	Zr^{4+}(ppm)	Cu^{2+}(ppm)
a	23.16	10.63
b	--	8.71
c	23.29	14.58

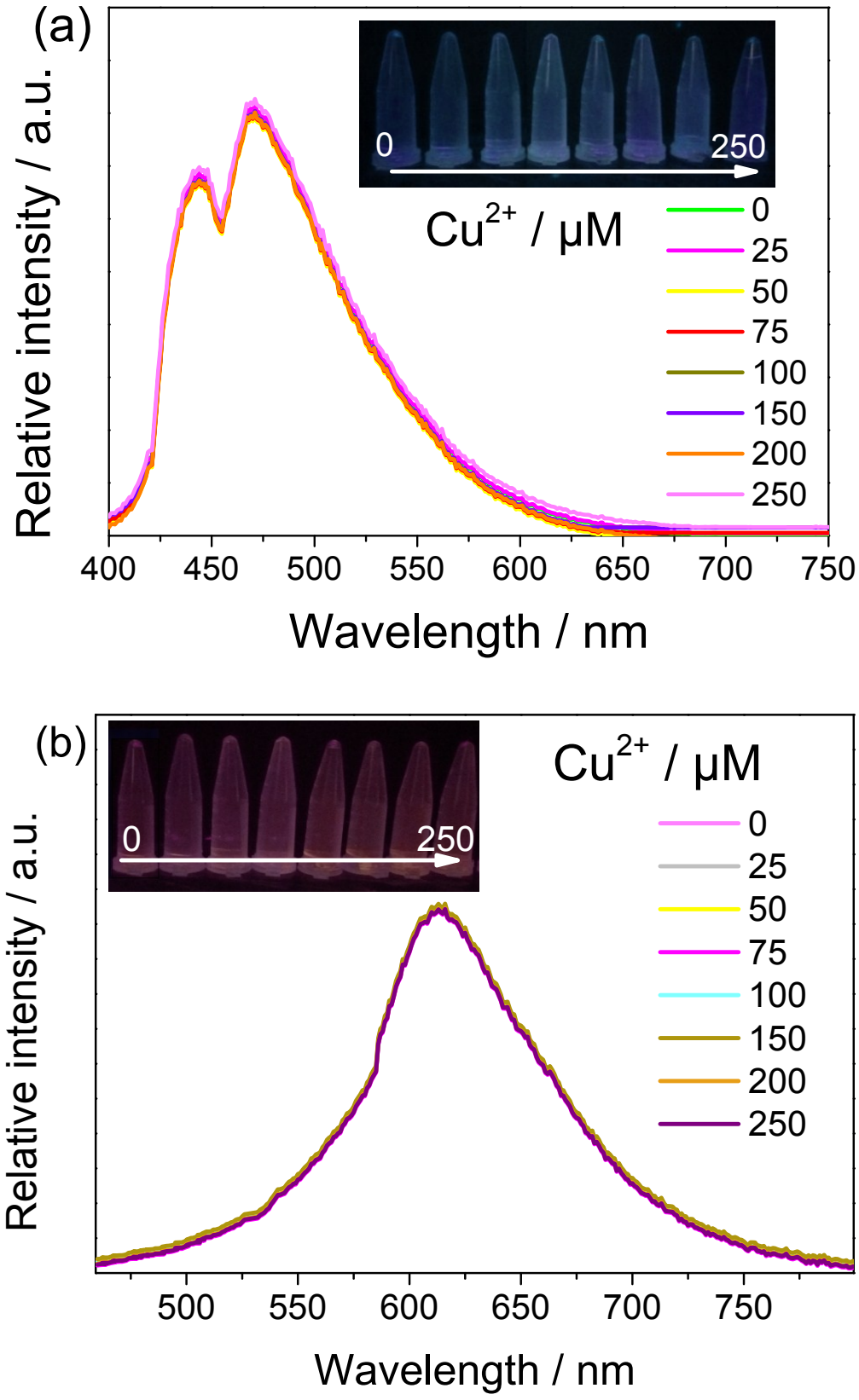

Fig. S13 Fluorescence emission spectra (λ_{ex} = 370 nm) of (a) UiO-66-$(COOH)_2$ and (b) R-BF-CQDs with the addition of Cu^{2+} ions.

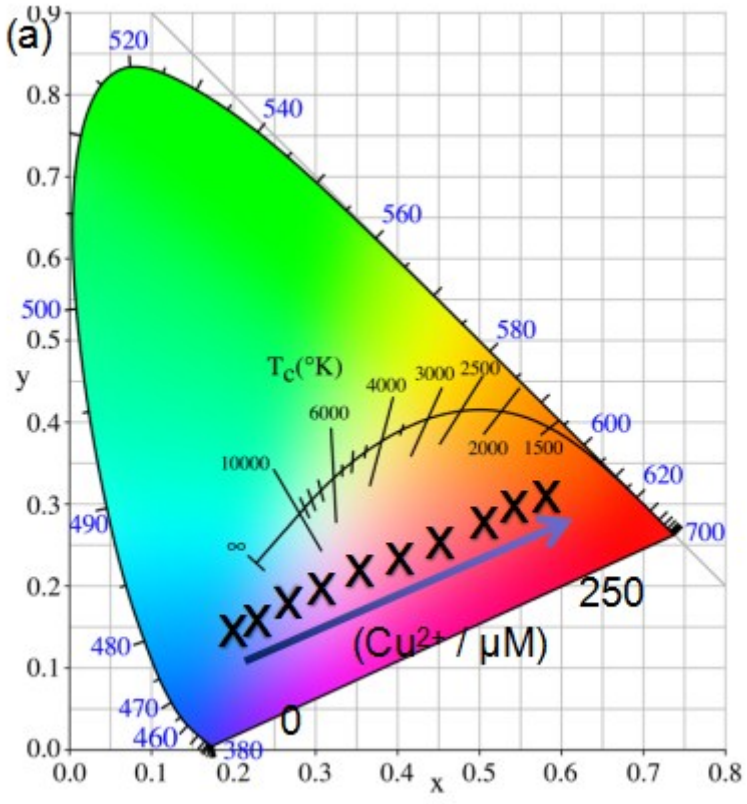

(b) Cu^{2+} / μM	X	Y
0	0.18	0.14
25	0.21	0.16
50	0.27	0.17
75	0.31	0.18
100	0.34	0.22
125	0.41	0.23
150	0.49	0.24
175	0.52	0.27
200	0.56	0.29
250	0.58	0.31

Fig. S14 (a) CIE chromaticity diagram of UiO-66-$(COOH)_2$ and R-BF-CQDs scattered in the aqueous solution containing different Cu^{2+} content excited at 370 nm. (b) Related values of CIE chromaticity diagram.

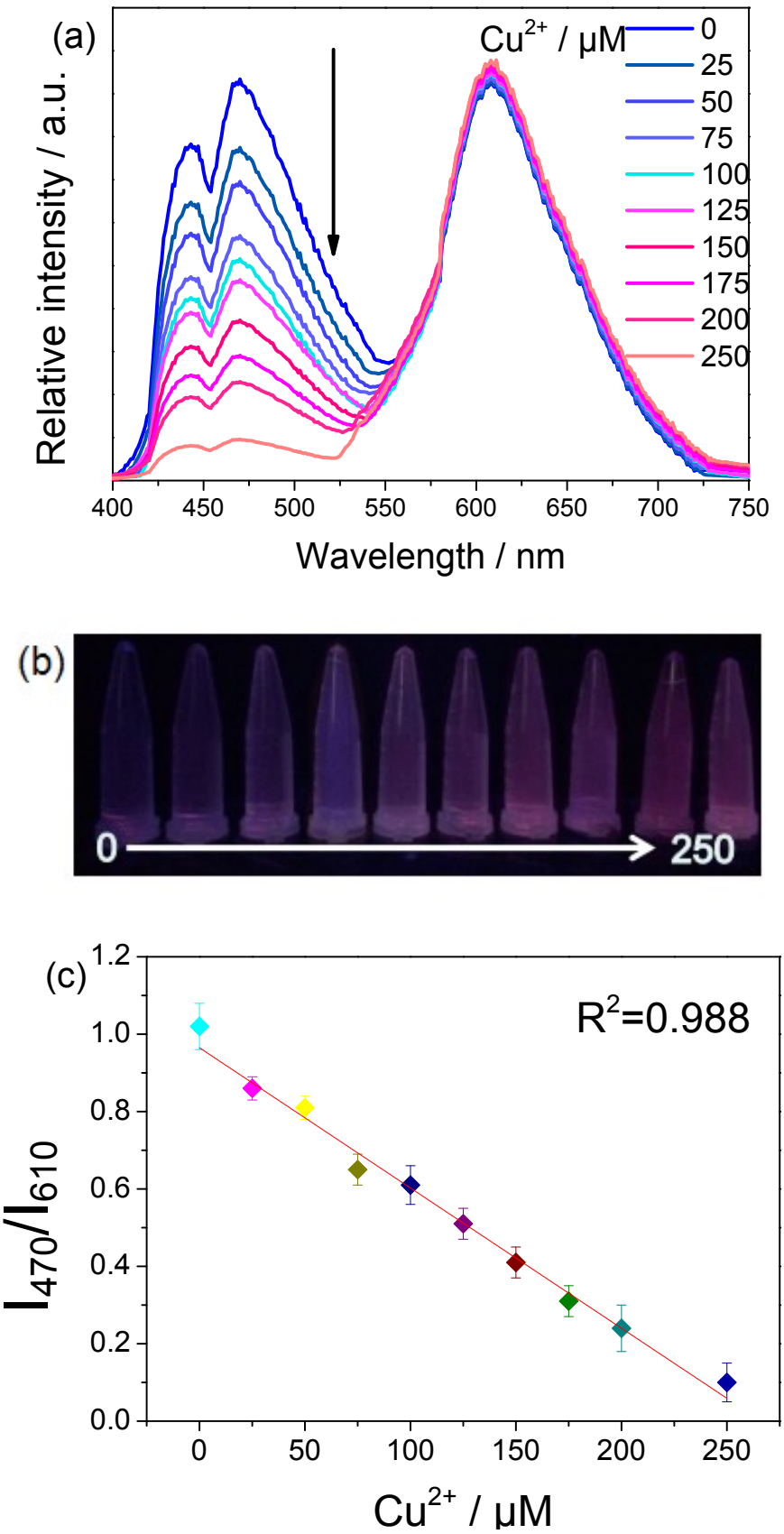

Figure. 15 (a) The change of fluorescence spectra of the mixture of UiO-66-$(COOH)_2$ and R-BF-CQDs with the addition of Cu^{2+} ions, initial ratio of I_{470}/I_{610} is 1:1. (b) Corresponding photos with color evolutions under a 365 nm UV lamp. (c) Calibration curve of fluorescence intensity ratio (I_{470}/I_{610}) of UiO-66-$(COOH)_2$ and R-BF-CQDs in the presence of various concentrations of Cu^{2+} under excitation at 370 nm.

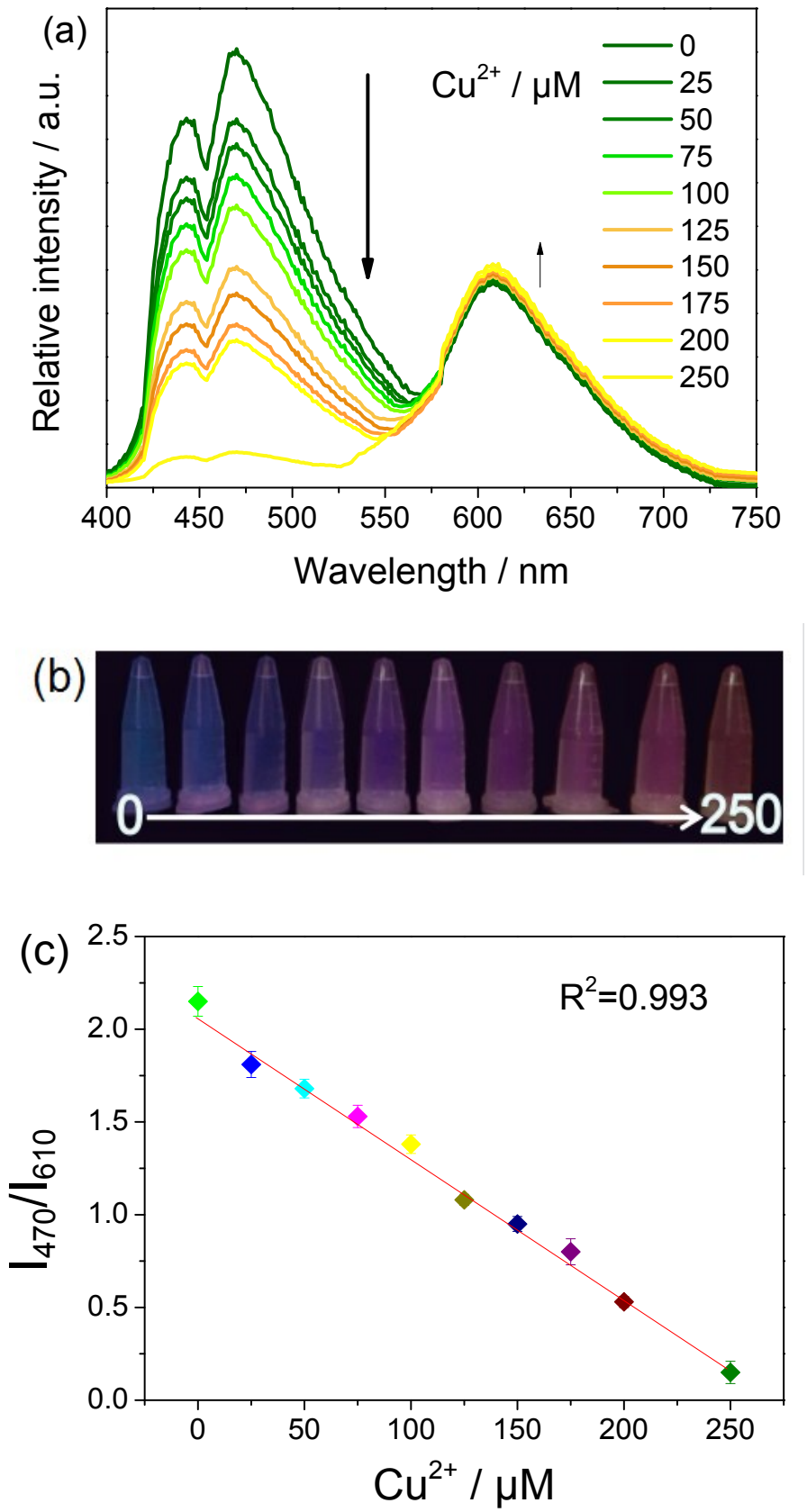

Figure. 16 (a) The change of fluorescence spectra of the mixture of UiO-66-$(COOH)_2$ and R-BF-CQDs with the addition of Cu^{2+} ions, initial ratio of I_{470}/I_{610} is 2:1. (b) Corresponding photos with color evolutions under a 365 nm UV lamp. (c) Calibration curve of fluorescence intensity ratio (I_{470}/I_{610}) of UiO-66-$(COOH)_2$ and R-BF-CQDs in the presence of various concentrations of Cu^{2+} under excitation at 370 nm.